Real-Time Implementation of PMU based Islanding Detection Schemes for Microgrids

Dinesh Rangana Gurusinghe, *Member, IEEE* and Dean S. Ouellette, *Senior Member, IEEE*

***Abstract*—A microgrid is a portion of a distribution network and is commonly designed to operate in parallel with the power grid or autonomously as a power island. Therefore, islanding detection is one of the key aspects of grid connected microgrids. In literature, performances of islanding detection methods are largely tested with offline simulation tools and only very limited attempts are made with real-time hardware-in-the-loop simulations. In this paper, a detailed microgrid model is implemented in a digital real-time simulator to assess five different islanding detection schemes with practical synchrophasor measurements. Performance of islanding detection schemes are evaluated in terms of accuracy, speed of detection and non-detection zone and quantitative results are presented.**

***Index Terms*—Microgrid, islanding detection, digital real-time simulation, phasor measurement unit (PMU), non-detection zone.**

I. Introduction

THE INTRODUCTION of distributed energy resources (DERs) alters conventional passive distribution system to an active network. This could reduce network losses, defer the investment costs required for network upgrades, reduce central generation reserve requirements, and improve overall power system reliability. In addition, active distribution systems can operate as a power island if DERs can operate in voltage and frequency control mode. A microgrid is a portion of an active distribution network designed to function as a single integrated system that can operate in parallel with the conventional centralized power grid or autonomously as a power island. The DERs commonly used in microgrids include wind, solar, synchronous generators driven by diesel, steam or hydro turbines, and combined heat and power plants.

Islanding is a condition in which a portion of the power system that contains both loads and generation particularly DERs, becomes isolated from the remainder of the power grid and continues to be in operation [1]. There are two types of islanding; intentional and unintentional. Intentional islanding is performed to improve the power quality and reliability or for maintenance purposes of the distribution network. Unintentional islanding occurs due to severe faults or equipment failure resulting in the opening of circuit breakers that interconnect the island with the rest of the power grid. Of course, unintentional islanding results in numerous safety and power quality issues as well equipment damages. Consequently, the IEEE standard 1547-2008 [2] recommends to isolate energized DERs within 2 s after an unintentional islanding event. Therefore, it is essential to detect unintentional islanding conditions as quickly as possible.

Islanding detection methods can be classified into two groups: local methods and remote methods. The former can be further classified as passive and active methods [3]. Phasor measurement unit (PMU) based islanding detection is one of the remote methods that offers fast, reliable, and accurate detection of islanding conditions under different operating conditions [4].

Islanding detection methods reported in literature are largely implemented on offline simulation tools and only very limited attempts are made with real-time hardware-in-the-loop (HIL) simulations. In HIL simulations, a portion of the power system is modeled in a software environment and interfaced with physical hardware devices using a real-time operating system [5]. This approach provides a cost effective and safe method to test the operation of physical devices before connected them to the actual power system [5]. Therefore, it is vital to test novel islanding detection techniques such as PMU based approaches in real-time HIL simulations to identify practical implementation issues and robustness of detection techniques to practical PMU measurements.

In this paper, a microgrid model with three DERs and their controls are implemented in a real-time digital simulator (RTDS®). The simulated microgrid model includes emulated PMUs that can stream C37.118 format synchrophasor measurements [8], [9]. Synchrophasor measurements are then fed to different islanding detection algorithms through a laboratory scale synchrophasor network to detect islanding conditions. Five different islanding detection algorithms, namely, over/undervoltage, over/underfrequency, rate of change of frequency (ROCOF), rate of change of relative phase angle (ROCORA) [6], phase angle difference vs. magnitude difference [7], are considered in this paper. The first three approaches are well-known passive islanding detection techniques based on local measurements and typically implemented in intelligent electronic devices (IEDs) as a protection function. The last two islanding detection techniques are proposed in recent literature and directly based on PMU measurements.

This paper is organized as follows. In Section II, five different islanding detection techniques stated before are briefly introduced. An example microgrid case and a laboratory scale test setup developed with the RTDS simulator are discussed in

D. R. Gurusinghe and D. S. Ouellette are with RTDS Technologies Inc., Winnipeg, MB, R3T 2E1, Canada (e-mail: dinesh@rtds.com; dean@rtds.com).

Section III. Section IV is devoted to analysis of results. It assesses different islanding detection algorithms. Finally, in Section V, the main contributions of this paper are highlighted.

II. ISLANDING DETECTION SCHEMES

In this section, five different islanding detection schemes are concisely discussed. The particular set of algorithms are chosen because they all can work with PMU measurements. The first three schemes discussed in this paper are passive methods and require one PMU installed in the vicinity of the microgrid. The last two methods need two PMUs; one installed in the grid side and the other installed in the microgrid side.

A. Overvoltage/undervoltage

Voltage magnitude at the microgrid side changes after an island is formed. If this variation exceeds or goes below a specified threshold range and persists for a certain period of time, then it is declared as an islanding condition. Fig. 1 shows the corresponding logic diagram.

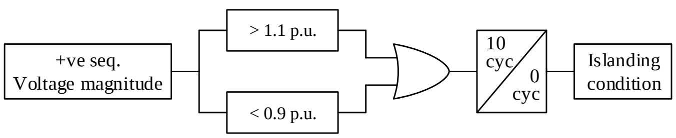

Fig. 1. Logic diagram : over/undervoltage scheme

In this study, positive sequence voltage magnitude obtained from the PMU at microgrid side is used. The upper and lower threshold limits are set to 1.1 p.u. and 0.9 p.u. respectively.

B. Overfrequency/underfrequency

When the microgrid is interconnected to the main power grid frequency variation is usually within ±1% tolerance. However, in case of islanding, the power mismatch between the generation and loads within the microgrid causes the frequency to rise above or drop below the allowed threshold for a specified period of time. The corresponding logic diagram is shown in Fig. 2.

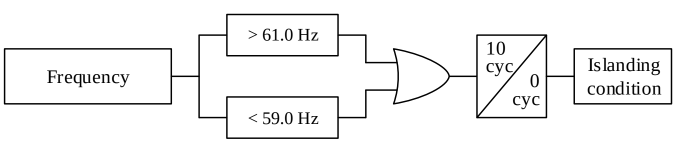

Fig. 2. Logic diagram : over/underfrequency scheme

In this scheme, frequency measurements are obtained from the PMU at microgrid side. The frequency threshold is limited to ±1.0 Hz of the nominal frequency (i.e. 59.0 ~ 61.0 Hz for a 60 Hz system) to account for islanding.

C. Rate of change of frequency (ROCOF)

The rate of change of frequency (ROCOF) method uses the first derivative of frequency as ROCOF is more sensitive to the power mismatch between the generation and loads within the microgrid. If the ROCOF of microgrid exceeds a specified threshold and persist for a certain period of time, then it is declared as an islanding condition. Fig. 3 shows the corresponding logic diagram. ROCOF measurements are obtained from the PMU at microgrid side and the threshold value is set to ±0.2 Hz/s.

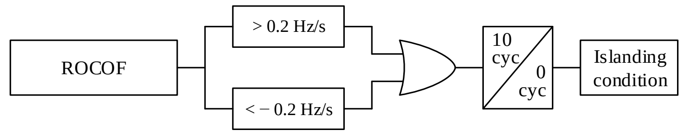

Fig. 3. Logic diagram : ROCOF scheme

D. Rate of change of relative phase angle (ROCORA)

Rate of change of relative phase angle (ROCORA) method is proposed in [6], where synchrophasors are used to estimate ROCORA between the microgrid and the main power grid. The ROCORA can be derived from two consecutive measurements as,

$$\begin{aligned}\mathrm{ROCOA}(n) = &\left(Vang_{M_1}(n) - Vang_{M_1}(n-1)\right)\cdot F_s \\ &- \left(Vang_{B_1}(n) - Vang_{B_1}(n-1)\right)\cdot F_s\end{aligned} \tag{1}$$

where $Vang_{M_1}$ and $Vang_{B_1}$ are the measured positive sequence voltage phase angles in the main grid and the vicinity of the microgrid and F_s is the PMU reporting rate given as frame/s. If the ROCORA exceeds a specified threshold and persist for a certain period of time, then it is declared as an islanding condition. The corresponding logic diagram is shown in Fig. 4.

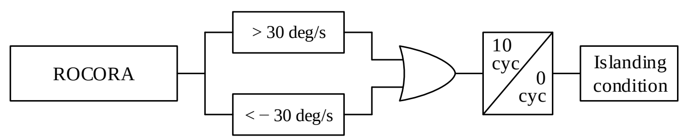

Fig. 4. Logic diagram : ROCORA scheme

In this paper, the threshold value is limit to ±30.0 deg/s to account for islanding.

E. Phase angle difference vs. magnitude difference

In [7], it is proposed to detect islanding condition by combing magnitude difference and phase angle difference between the microgrid and the main power grid. The magnitude difference, ΔMag and phase angle difference, ΔAng can be estimated as,

$$\Delta Mag = Vmag_{M_1} - Vmag_{B_1} \tag{2}$$

$$\Delta Ang = Vang_{M_1} - Vang_{B_1} \tag{3}$$

where $Vmag_{M_1}$ and $Vang_{M_1}$ are voltage magnitude and phase angle of the PMU in the main power grid while $Vmag_{B_1}$ and $Vang_{B_1}$ are corresponding measurements of the PMU in the vicinity of the microgrid. A threshold of this algorithm is defined as an ellipse on the ΔAng vs. ΔMag plane as shown in Fig. 5 [7].

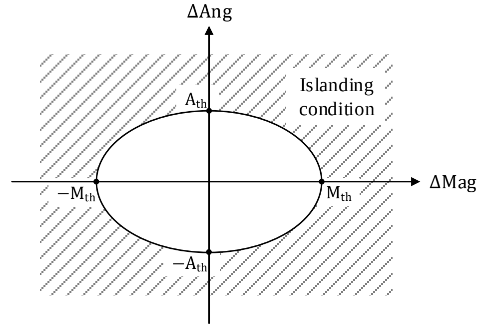

Fig. 5. Phase angle difference vs. magnitude difference plane

When the microgrid is interconnected to the main power grid magnitude and phase angle differences are small and the ΔAng-ΔMag trajectory lies within the ellipse. However, magnitude and phase angle variations are significant after an island is formed and therefore, the trajectory moves away from the ellipse. The corresponding logic diagram is shown in Fig. 6.

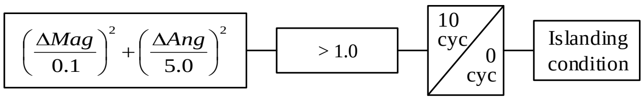

Fig. 6. Logic diagram : ΔAng vs. ΔMag scheme

In this scheme, positive sequence voltage phasors are used. The threshold values M_{th} and A_{th} are set to 0.1 p.u. and 5.0 deg respectively.

III. MICROGRID CASE AND TEST SETUP

A modified version of CIGRE C6.04.02 benchmark North American medium voltage (MV) distribution network [10] and topology of the microgrid structure is shown in Fig. 7.

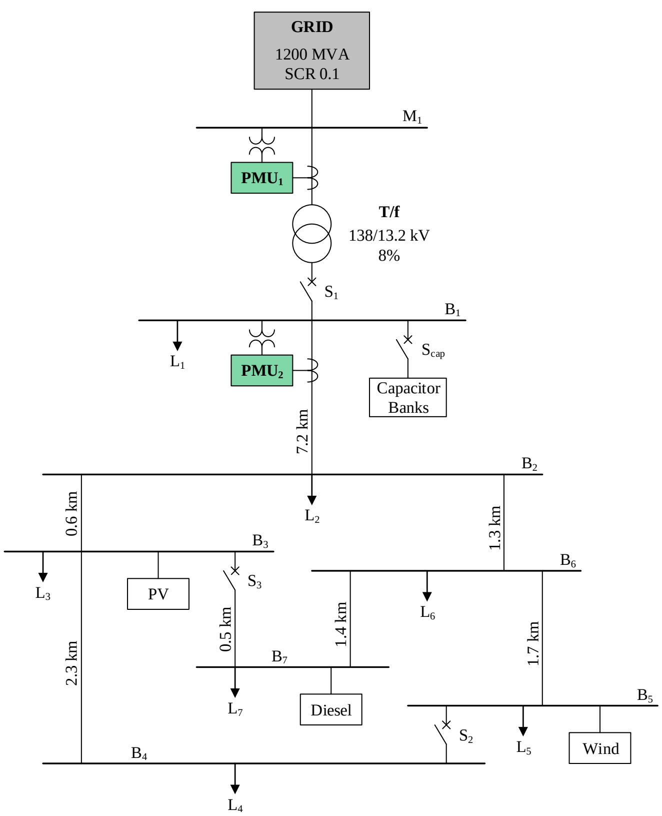

Fig. 7. Topology of the Microgrid; locations of the PMUs are indicated

The microgrid is connected to the 138 kV main network through a 25 MVA, 138/13.2 kV Δ-Y transformer with 8% impedance [11]. The DERs in the microgrid include a 1.74 MW photovoltaic (PV) system connected to bus B_3, a 2.0 MW doubly-fed induction generator (DFIG) wind turbine system connected to bus B_5, and a 5.5 MVA diesel generator connected to bus B_7. Five switched capacitors banks rated at 500 MVar each are connected at bus B_1 to provide reactive power support. The microgrid is interconnected using a circuit breaker S_1 and disconnector switches S_2 and S_3 are kept open to maintain a radial network. The total loading of the microgrid is 7.39 MW and 2.936 MVar [11]. It is assumed that the two PMUs are installed at bus M_1 (grid side) and bus B_1 (in the vicinity of microgrid). It is further assumed that the two PMUs are located in the same substation and stream their outputs to a local phasor data concentrator (PDC), which is also located in the same substation.

In order to investigate performances of PMU based islanding detection schemes, a laboratory scale test setup shown in Fig. 8 is developed with the RTDS simulator.

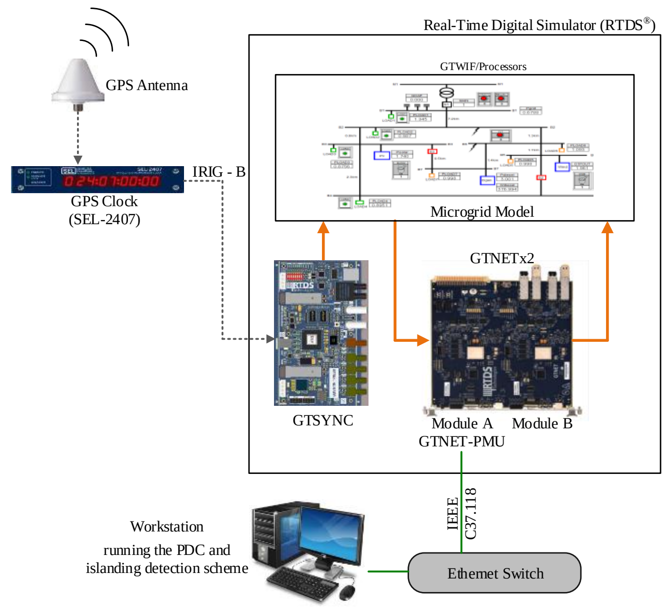

Fig. 8. Connection setup with the RTDS simulator and the GTNET-PMUs

The RTDS simulator used in this test setup is equipped with a GTNETx2™ card, which is basically a network protocol converter [5]. The GTNETx2 card is capable of running two network protocols simultaneously and the PMU protocol can emulate up to 8 PMUs [5]. For the test setup shown in Fig. 8, PMU protocol is selected to run on module A and two PMUs are enabled. P-class PMU algorithm available in the RTDS simulator, at a reporting rate of 60 frames/s is selected for both PMUs as it is preferred for the applications requiring fast responses such as islanding detection [12]. A global positioning system (GPS) clock is used to provide time signal to the RTDS simulator via a GTSYNC™ card. The synchrophasor measurements are collected by the openPDC™ v2.0 [13] PDC and provided to the islanding detection algorithms.

IV. SIMULATION RESULTS

Under steady-state condition, PV and wind systems were operated as constant PQ sources at unity power factor at their rated power (i.e. 1.74 MW and 2.0 MW respectively). In grid-connected mode, the microgrid was importing 0.659 MW and 2.236 MVar from the main grid and the diesel generator operated in a droop control and produced 3.0 MW and 1.736 MVar. All five capacitor banks were kept disconnected. The system was islanded by opening the circuit breaker S_1. Blue trajectories in Fig. 9 illustrate variations of five islanding detection indicators discussed in Section II. The green vertical line shows the coordinated universal time (UTC) of 21:50:31.464 when the system was islanded. Red horizontal lines display threshold limits. Fig. 10 shows the ΔAng-ΔMag trajectory.

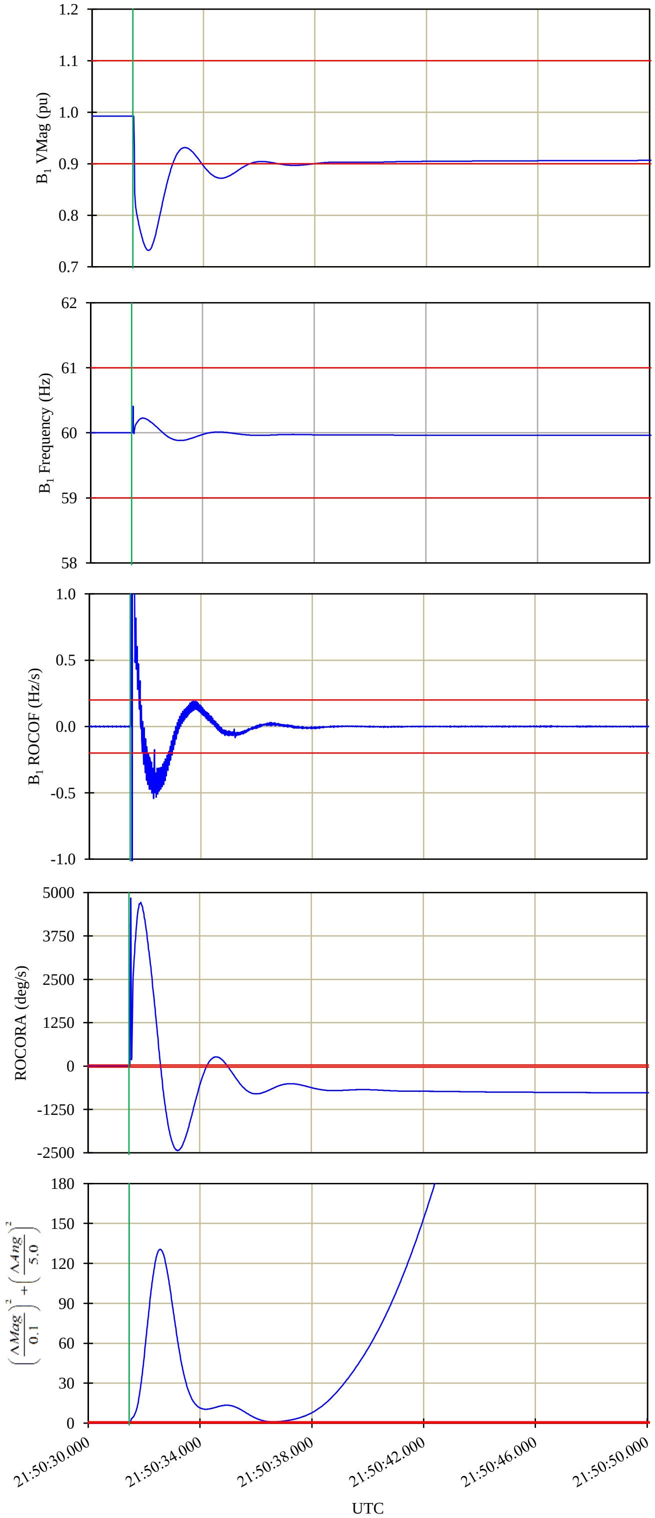

Fig. 9. Variations of five islanding detection indicators : base-case

Except the under/overfrequency scheme, all other four schemes accurately detected the islanding condition and the response times were around 200 ms. Exact response times of the base-case can be found in Table I.

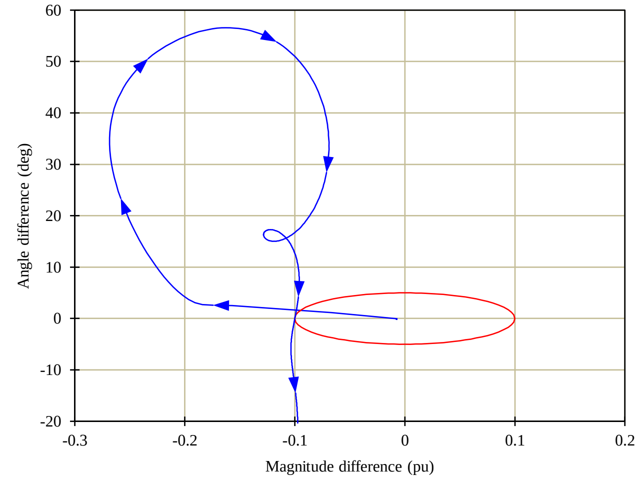

Fig. 10. ΔAng-ΔMag trajectory : base-case

TABLE I: RESPONSE TIMES : BASE-CASE

	Response time (ms)				
	Under/over voltage	Under/over frequency	ROCOF	ROCORA	ΔAng vs. ΔMag
$P_{imbalance}$ = 8.9% $Q_{imbalance}$ = 56.3%	219	Not detect	202	202	219

The percentage power imbalance of the microgrid is defined as [14],

$$P_{imbalance} = \frac{\pm P_{grid}}{P_{grid} + P_{pv} + P_{wind} + P_{diesel}} \tag{4}$$

$$Q_{imbalance} = \frac{\pm Q_{grid}}{Q_{grid} + Q_{pv} + Q_{wind} + Q_{diesel}} \tag{5}$$

The positive sign indicates the microgrid is importing power from the main grid and the negative sign indicates the microgrid is exporting power to the main grid. The calculated $P_{imbalance}$ and $Q_{imbalance}$ values for the base-case are 8.9% and 56.3% respectively.

The microgrid loads and generations were exactly matched to set both $P_{imbalance}$ and $Q_{imbalance}$ values to zero. The system was islanded by opening the circuit breaker S_1 when the UTC was of 15:54:42.244. Obviously, this is the most difficult situation (worst-case) to detect the islanding condition. Fig. 11 and Fig. 12 illustrate variations of five islanding detection indicators and the ΔAng-ΔMag trajectory respectively.

All three passive schemes failed to detect the islanding condition. The ROCORA and the ΔAng vs. ΔMag schemes successfully detected the islanding condition, however, the ΔAng vs. ΔMag scheme was very slow. Table II shows the corresponding response times.

TABLE II: RESPONSE TIMES : WORST-CASE

	Response time (ms)				
	Under/over voltage	Under/over frequency	ROCOF	ROCORA	ΔAng vs. ΔMag
$P_{imbalance}$ = 0.0% $Q_{imbalance}$ = 0.0%	Not detect	Not detect	Not detect	306	8189

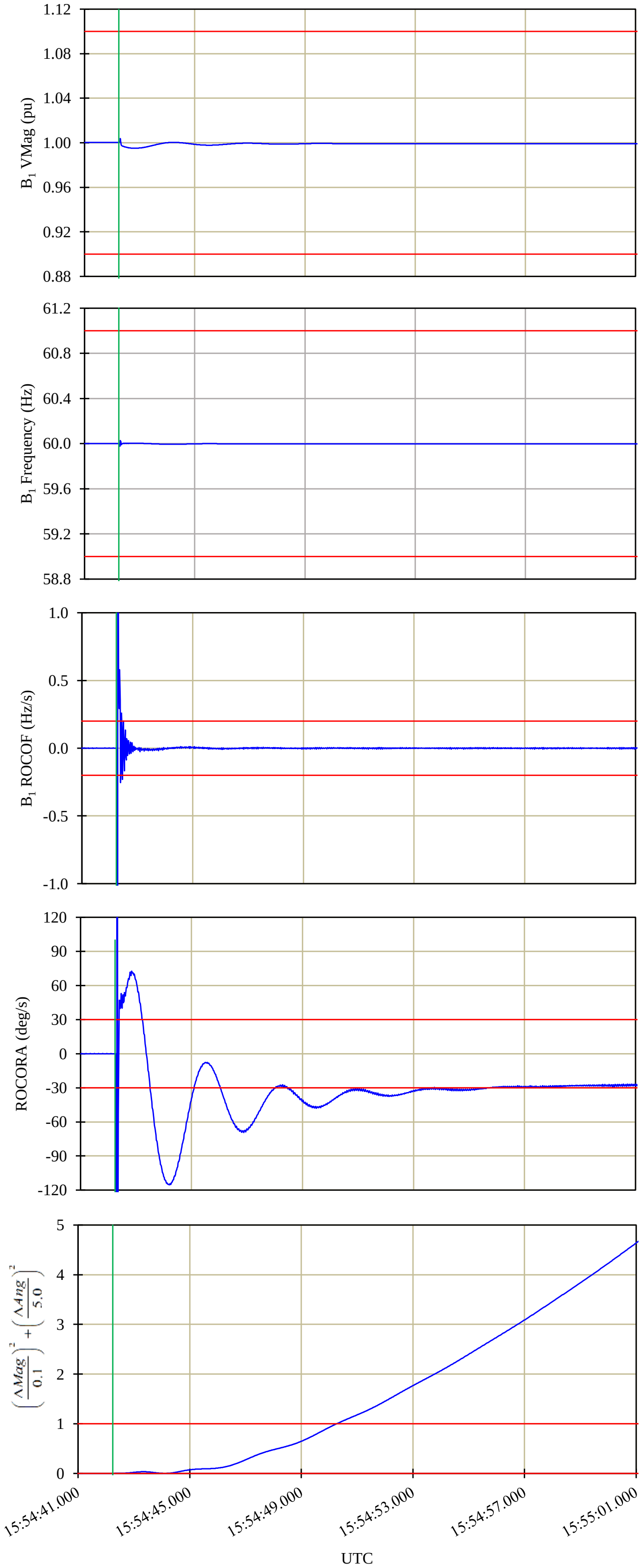

Fig. 11. Variations of five islanding detection indicators : worst-case

In order to investigate the non-detection zone (NDZ) of different islanding detection schemes, $P_{imbalance}$ and $Q_{imbalance}$ values of the microgrid were varied. Table III presents the response times of islanding detection schemes when $Q_{imbalance}$ was kept zero and $P_{imbalance}$ values were varied from –40% to 40%.

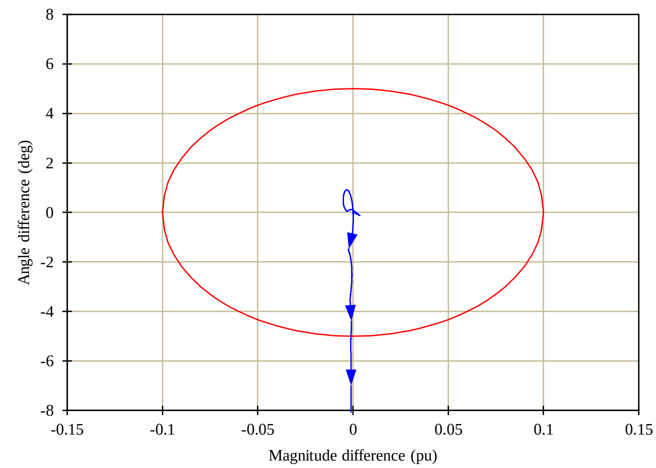

Fig. 12. ΔAng-ΔMag trajectory : worst-case

TABLE III: RESPONSE TIMES : $Q_{imbalance} = 0$

$P_{imbalance}$ (%)	Response time (ms)				
	Under/over voltage	Under/over frequency	ROCOF	ROCORA	ΔAng vs. ΔMag
–40	Not detect	Not detect	193	193	210
–30	Not detect	Not detect	201	201	217
–20	Not detect	Not detect	196	197	247
–10	Not detect	Not detect	414	205	355
0	Not detect	Not detect	Not detect	306	8189
10	Not detect	Not detect	Not detect	206	289
20	1113	Not detect	347	196	213
30	380	2547	200	200	217
40	267	2200	196	197	214

The same test was repeated while $P_{imbalance}$ was kept zero and $Q_{imbalance}$ values were varied from –40% to 40%. Simulation results are shown in Table IV.

TABLE IV: RESPONSE TIMES : $P_{imbalance} = 0$

$Q_{imbalance}$ (%)	Response time (ms)				
	Under/over voltage	Under/over frequency	ROCOF	ROCORA	ΔAng vs. ΔMag
–40	Not detect	Not detect	199	200	450
–30	Not detect	Not detect	Not detect	206	489
–20	Not detect	Not detect	Not detect	205	555
–10	Not detect	Not detect	Not detect	199	2082
0	Not detect	Not detect	Not detect	306	8189
10	Not detect	Not detect	Not detect	196	796
20	Not detect	Not detect	Not detect	194	444
30	Not detect	Not detect	Not detect	192	392
40	293	Not detect	193	193	243

According to the simulation results the NDZ of three passive schemes is significant. The under/overfrequency scheme shows worst performances. The ROCOF scheme is the best among passive schemes, however, shows very poor performances when no active power exchange between the microgrid and the main grid. The ROCORA and the ΔAng vs. ΔMag schemes showed much better performances compared with passive schemes. However, the response time of the ΔAng vs. ΔMag scheme is high when power exchange between the microgrid and the main grid small and therefore, offers less advantages.

V. Conclusion

In this paper, five different islanding detection schemes were assessed with practical PMU measurements. A detailed microgrid model with DERs and PMUs was implemented in the RTDS simulator. Synchrophasor measurements were fed to islanding detection schemes through a laboratory scale synchrophasor network. Real-time simulations were carried out to assess performances of islanding detection schemes. Simulated test cases revealed that the NDZ of passive methods is significant and their response time are high when small amount of power exchanged between the microgrid and the main grid. The ROCORA scheme is the best approach in terms of speed and it was able to detect the islanding condition under all tested circumstances. In addition, the proposed laboratory scale synchrophasor network with the RTDS simulator will be a helpful tool to study other practical issues of microgrids as well as synchrophasor applications.

VI. References

[1] F. Katiraei, M. R. Iravani, and P. F. W. P. Lehn, "Micro-grid autonomous operation during and subsequent to islanding process," *IEEE Trans. Power Del.*, vol. 20, no. 1, pp. 248–257, Jan. 2005.

[2] *IEEE standard for interconnecting distributed resources with electric power systems*, IEEE Std 1547.2-2008, Apr. 2009.

[3] C. Li, C. Cao, Y. Cao, Y. Kuang, L. Zeng, and B. Fang, "A review of islanding detection methods for microgrid," *Renewable and Sustainable Energy Reviews*, vol. 35, pp. 211-220, 2014.

[4] R. Franco, C. Sena, G. N. Taranto, and A. Giusto, "Using synchrophasors for controlled islanding-A prospective application for the Uruguayan power system," *IEEE Trans. Power Syst.*, vol. 28, no. 2, pp. 2016-2024, May 2013.

[5] Real Time Digital Simulator (RTDS) Manuals and Documentation, RTDS Technologies, Winnipeg, MB, Canada, 2015.

[6] J. Y. Zhang and C. M. Bush, "PMU based islanding detection to improve system operation," in *Proc. IEEE Power Eng. Soc. General Meeting*, Boston, MA, USA, July 2016, pp. 1-5.

[7] J. Cardenas, G. Mikhael, J. Kaminski and I. Voloh, "Islanding detection with Phasor Measurement Units," in *Proc. of 67th Annual Conference for Protective Relay Engineers*, College Station, TX, USA, 2014, pp. 229-241.

[8] *IEEE standard for synchrophasors for power systems*, IEEE Std C37.118-2005, Mar 2006.

[9] *IEEE standard for synchrophasor data transfer for power systems*, IEEE Std C37.118.2-2011, Dec. 2011.

[10] *Benchmark Modeling and Simulation for Analysis, Design, and Validation of Distributed Energy Systems*, CIGRE C6.04.02 Task Force, Sep. 2006.

[11] O. Nzimako, "Real-time simulation of a microgrid system with distributed energy resources," M.Sc. thesis, Dept. Elect. & Comp. Eng., Univ. Manitoba, Winnipeg, MB, Canada, 2015.

[12] *IEEE Standard for Synchrophasor Measurements for Power Systems*, IEEE Std C37.118.1-2011, Dec. 2011.

[13] OpenPDC, Grid Protection Alliance [Online]. Available: http:// open-pdc.codeplex.com.

[14] N. W. A. Lidula, "Determination of requirements for smooth operating mode transition and development of a fast islanding detection technique for microgrid," Ph.D. thesis, Dept. Elect. & Comp. Eng., Univ. Manitoba, Winnipeg, MB, Canada, 2012.

VII. Biographies

Dinesh Rangana Gurusinghe (S'11, M'17) received the B.Sc. (Eng.) degree from the University of Moratuwa, Katubedda, Sri Lanka, in 2003, the M.Eng. degree from the Asian Institute of Technology, Bangkok, Thailand, in 2010, and the Ph.D. degree from the University of Manitoba, Winnipeg, MB, Canada, in 2017, all in Electrical Engineering. He was the recipient of multiple academic awards during his graduate studies.

He worked as an Electrical Engineer at Cruickshanks Ceylon Ltd, Sri Lanka and Ceylon Electricity Board, Sri Lanka from 2003 to 2008. Since 2015 he is working at RTDS Technologies Inc., Canada as a Simulation Specialist. He is a Corporate Member and a Chartered Engineer in the Institution of Engineers, Sri Lanka.

His main research areas are synchrophasor measurements and their applications in power system, real-time digital simulation, power system protection and automation, power system stability, and power system operation. Dr. Gurusinghe has co-authored more than 20 journal publications, conference papers, and technical reports.

Dean S. Ouellette graduated from the Red River Community College in Winnipeg, MB, Canada with a Diploma in Electrical Engineering Technology, in 1986.

His employment experience includes Manitoba Hydro, British Columbia Hydro, Schweitzer Engineering Labs, NxtPhase T&D, and RTDS Technologies Inc., Canada. Mr. Ouellette is currently the Manager for Protection and Automation products at RTDS and is an active participant in IEEE/PSRC working groups and standards development.